Adsorptive Removal of Methylene Blue by Commercial Coconut Shell Activated Carbon

Ramlah Abd Rashid[1], Mohd Azlan Mohd Ishak[2*] and Kasim Mohammed Hello[3]

[1]Faculty of Applied Sciences, Universiti Teknologi MARA, 40450 Shah Alam, Selangor
[2]Faculty of Applied Sciences, Universiti Teknologi MARA, 02600 Arau, Perlis
[3]Chemistry Department, College of Science, Al Muthanna University, Iraq
[*]E-mail: azlanishak@perlis.uitm.edu.my

Received: 1 February 2018
Accepted: 29 June 2018

ABSTRACT

This paper shows the using of commercial coconut shell activated carbon (CCS-AC) as an alternative adsorbent for the removal of methylene blue (MB) from aqueous solution. The physicochemical properties of the CCS-AC were undertaken using Fourier Transform Infrared Spectroscopy (FTIR), Scanning Electron Microscopy (SEM) and pH Point of Zero Charge (pH_{pzc}) method. Batch adsorption experiments were conducted to study the influence of adsorbent dosage (0.02 – 0.50 g), pH (3 – 10), MB concentration (25 – 400 mgL^{-1}) and contact time (0 – 36 hours) on the adsorption of the MB. The kinetic adsorption was well described by the Pseudo Second Order model and the Langmuir model described the adsorption behavior at equilibrium. The maximum adsorption capacity (q_{max}) of CCS-AC obtained was 149.25 mg/g at 303 K.

Keywords: *commercial activated carbon, coconut shell, methylene blue, adsorption*

INTRODUCTION

In recent decades, society has become highly alarmed with protection of the environment. Water pollution has been under constant debate since it is considered as the most concern environmental problem among others [1]. Effluents from various industrial branches are settled into the water bodies mainly are from dyes manufacturing such as; textile, leather, rubber, plastics, cosmetics and pharmaceutical [2].

Basic dyes are cationic due to the positive charge delocalized throughout the chromophoric system. It is named because of it affinity to basic textile materials with negatively charged functional groups [3]. Methylene blue (MB) is an example of basic dye which has been shown to have harmful effects on living organisms on short periods of exposure [4]. Although it is not regarded as acutely toxic, it presence can cause aesthetic and ecological problems [5]. MB blocked the transmission of sunlight into water bodies hence affecting photosynthesis of aquatic flora and oxygenation of water reservoirs. As in health viewpoint, MB has carcinogenic properties that can lead to several diseases such as allergic dermatitis and skin irritation [6]. Meanwhile, the ingestion of MB through mouth creates a burning sensation and may cause nausea, vomiting, diarrhea and gastritis [7].

Several water treatments have been developed to remove dyes from wastewater, such as; membrane separation [8], bioremediation [9], electrochemical degradation [10], cation exchange membranes [11], Fenton chemical oxidation [12] and photocatalysis [13, 14]. Nevertheless, some of the above treatments pose drawbacks of being expensive, production of toxic sludge and involve complex procedure [15]. Adsorption of dyes using activated carbon (AC) is one of the frequently applied methods for water purification and water reuse [16]. This technique has gained much attention due to the advantages such as; convenience of operation and selectivity, high performance, superior design flexibility and no formation of harmful by-products [17].

Activated carbon (AC) is a carbonaceous materials [18], with high porosity [19–23], high physicochemical stability [24], high adsorptive capacity [25], high mechanical strength [26, 27], high degree of surface reactivity [28, 29], with immense surface areas [30, 31] which can be differentiated from elemental carbon by the oxidation of the carbon atoms that found at the outer and inner surfaces [32]. AC is among the best option in wastewater treatment due to its ability to adsorb various types of pollutants from the media such as dyes, heavy metal, pesticides and gases [33]. There are a few factor may affect adsorption capacity such as; source of raw materials, preparation and treatment conditions, surface chemistry, surface charge, pores structure, surface areas and accessibility of the pollutants to the inner surface of the adsorbent [34].

Coconut is a versatile plant species. It has been widely used as a source of food, fuel wood, drink, edible oil, fibre, animal feed and construction materials. Although coconut industry supports the economic growth of Malaysia, it generates large amounts of wastes. Every year, huge quantities of coconut waste are produced and left in the plantation floor which aggravates fungi and pest infestation. The disposal of the coconut wastes remains a serious problem since it can negatively affect the environment. Thus, these materials can be converted into a value-added adsorbent and a potential precursor for the preparation of AC.

MATERIALS AND METHODS

The commercial coconut shell activated carbon (CCS-AC) was purchased from Tan Meng Keong Sdn. Bhd, Selekoh, Perak, Malaysia. It was washed several times with distilled water to remove dirt followed by drying at 110°C for 24 hours. The dried CCS-AC was ground and sieved to the size between 250-500 μm. Finally, the CCS-AC powder was stored in an airtight container for further use. Methylene blue (MB) with molecular formula of $C_{16}H_{18}ClN_3S.xH_2O$ and molecular weight of 319.86 $gmol^{-1}$ supplied by R&M Chemical was used as an adsorbate model for adsorption studies. A 1000 mgL^{-1} stock solution of MB was prepared by dissolving 1.0 g of MB powder in distilled water. The stock solution was used to prepare a series of MB concentrations ranging from 25 to 400 mgL^{-1}. Solution of different pH was prepared using HCl or NaOH (HmbG). All chemicals were used without further purification.

The characterizations of CCS-AC were determined by FTIR (Perkin Elmer, Spectrum One) in the 4000 cm^{-1}-500 cm^{-1} wavenumber range. The surface physical morphology was examined by using Scanning Electron Microscopy (SEM; SEM-EDX, FESEM CARL ZEISS, SUPKA 40 VP). The pH at the point of zero charge (pH_{pzc}) was estimated using a pH meter (Metrohm, Model 827 pH Lab, Switzerland), as described by Lopez-Ramon et al. [35]. The adsorption experiments of MB onto CCS-AC were performed in a set of 250 mL conical flasks containing 100 mL of MB solution. The flasks were capped and agitated in water bath shaker (Memmert, water bath, model WNB7-45, Germany) at fixed shaking speed of 110 $strokemin^{-1}$ and 303 K until equilibrium was achieved. Batch adsorption experiments were carried out by varying several experimental variables such as adsorbent dosage (0.02 to 0.50 g), pH (3 to 10), MB concentration (25 to 400 mgL^{-1}) and contact time (0 to 36 hours) to determine the best uptake conditions for adsorption. The pH of MB solution was adjusted by adding either 0.10 $molL^{-1}$ HCl or NaOH. After mixing of the CCSAC-MB system, the supernatant was collected using a 0.20 μm Nylon syringe filter and the concentrations of MB were monitored at a different time interval using a HACH DR 2800 Direct Reading Spectrophotometer at the maximum wavelength (λ_{max}) of absorption at 661 nm. As for the thermodynamic studies, the same procedures were repeated and applied at 313 and 323 K with the other parameters keep constant. The blank test was carried out in order to account for colour leached by the adsorbent and adsorbed by the glass containers. Blank runs with only the adsorbent in 100 mL of doubly distilled water and 100 mL of dye solution without any adsorbent were conducted simultaneously at similar conditions. The adsorption capacity at equilibrium, q_e (mgg^{-1}) and the percent of colour removal, *CR* (%) of MB were calculated using Eqs. (1) and (2).

$$q_e = \frac{(C_o - C_e)\ V}{W} \qquad (1)$$

$$CR\,\% = \frac{(C_o - C_e)}{C_o} \times 100 \qquad (2)$$

where C_o and C_e (mgL^{-1}) are the initial and equilibrium concentrations of MB, respectively, *V* (L) is the volume of the solution and *W* (g) is the mass of dry adsorbent used.

RESULTS AND DISCUSSION

Physical Properties of CCS-AC

The results of physical properties of CCS-AC are presented in Table 1.

Table 1: Physicochemical Characterization of CCS-AC

Physical Properties	Values
Bulk Density (gmL^{-1})	0.47
Ash Content (wt %)	3.26
Moisture Content (wt %)	0.18
Iodine Number (mgg^{-1})	516.70

The strength of adsorbent is related to the amount of fibre content in it [36]. Bulk density analysis was conducted to determine the mechanical strength of CCS-AC. In this work, the CCS-AC had a low density, meaning that, there was only a small amount of MB that the CCS-AC can hold per unit volume. Meanwhile, ash is an additive, contains mineral constituents, which become highly concentrated during activation process. The threshold limit of ash content in adsorbent should not exceed 15.0% [37]. Ash content of CCS-AC was low (3.26%), indicates that CCS-AC has less extractives with little or no wax and resin [38]. Iodine number analysis is the simplest parameter to define the quality of AC. An excellent AC is expected to have iodine value from 900 mgg^{-1} and above. The iodine number of CCS-AC was reported to be moderately high with 516.70 mgg^{-1}.

FTIR Analysis of CCS-AC

The patterns of adsorption were associated with the availability of the active functional groups and bonds on the adsorbent surface. FTIR spectroscopy elucidates the structural and compositional information on the active functional groups that are present in the adsorbent. FTIR spectrum of CCS-AC before adsorption (Fig. 1a) showed various functional groups, in agreement with their respective wavenumber (cm^{-1}) position.

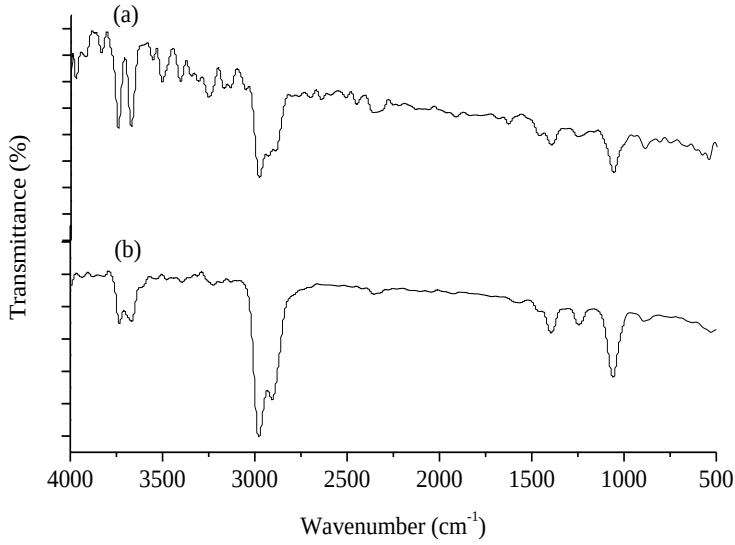

Figure 1: FTIR spectra of CCS-AC (a) before MB adsorption and (b) after MB adsorption

The broad band at ~3500 cm^{-1} was assigned to the overlapping of the stretching vibrations of the hydroxyl (O−H) and amine (N−H) groups [39] while band around ~3000 cm^{-1} was due to carboxylic acid O−H stretching [40]. The absorptions peaks ~1000 cm^{-1} were observed for oxidized carbon materials and were assigned to C–O and/or C–O–C stretching in acids, alcohols, phenols, ethers and/or esters groups [41]. Thus, the FTIR spectrum of CCS-AC before adsorption indicates that the external surface of CCS-AC is rich with various functional groups, containing oxygen of carboxylic and carbonyl species. These active groups on CCS-AC surface are responsible for enhancing the adsorption of MB due to the electrostatic interaction. After MB adsorption (Fig. 1b), the band shifted and became more pronounced in which suggest the interaction of MB molecules with the functional groups of CCAS-AC.

Surface Morphology of CCS-AC

SEM analysis was carried out to visualise the morphology of CCS-AC before adsorption and its changes after adsorption of MB had taken place.

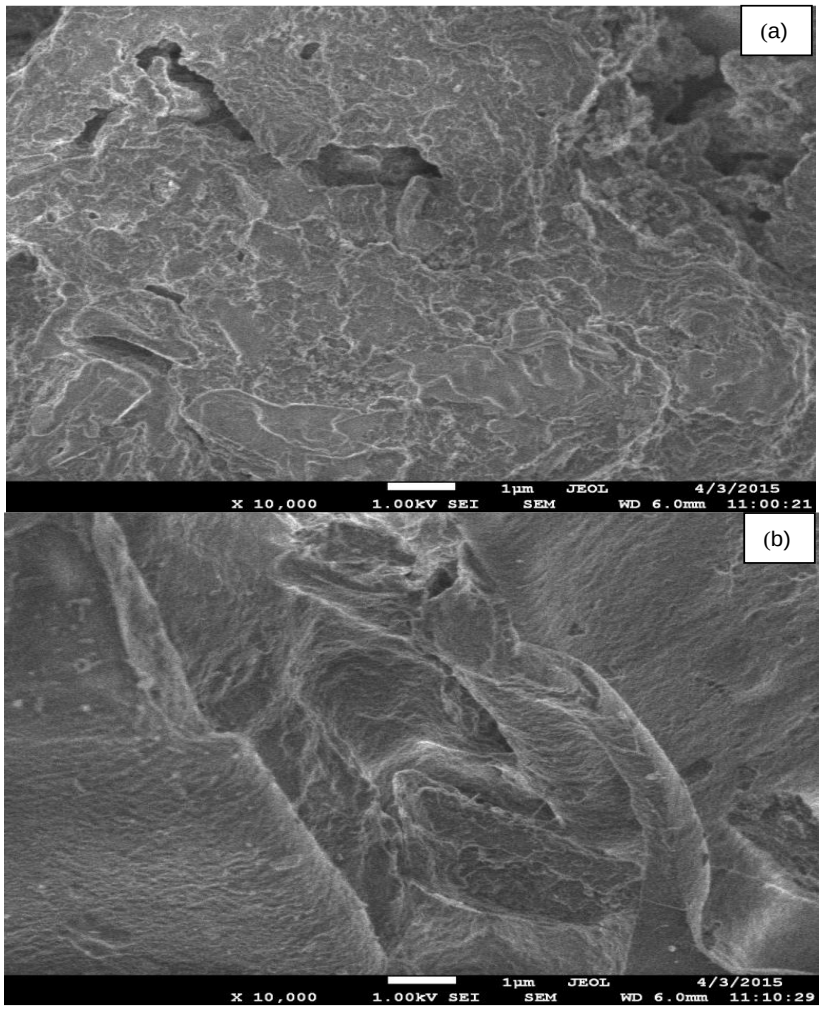

Figure 2: SEM micrograph of CCS-AC (a) before MB adsorption (b) after MB adsorption

The SEM images of CCS-AC before and after MB adsorption are shown in Fig. 2a and 3b, respectively. As seen in Fig. 2a, the external surface of CCS-AC displays a rough texture distributed over the surface. After MB adsorption, the CCS-AC surface was transformed to be more compact and smoother due to the filling of MB molecules on the CCS-AC surface.

Point of Zero Charge (pH_{pzc}) of CCS-AC

The point of zero charge (pH_{pzc}) analysis was studied to estimate the pH at which the net charge of the surface of adsorbent is zero. Fig. 3 shows the pH_{pzc} plot performed at pH ranged from 3 to 10 and pH_{pzc} of CCS-AC was obtained at 6.5.

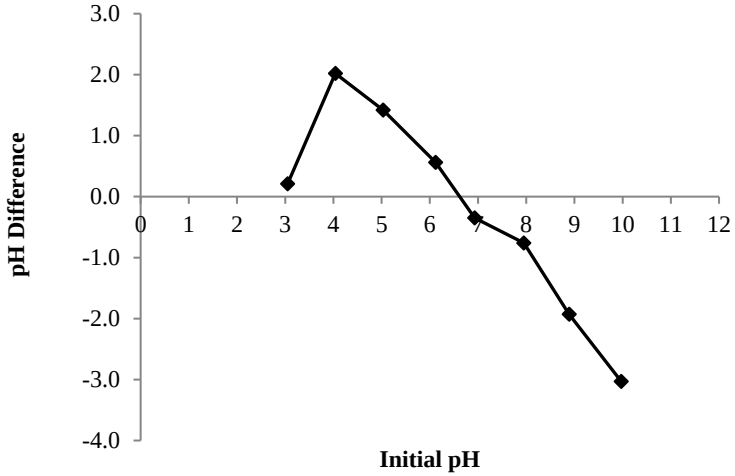

Figure 3: pH_{pzc} of CCS-AC suspensions

In general, MB adsorption is favoured at pH > pH_{pzc}, due to the presence of functional groups such as OH−, COO−groups while anionic dye adsorption is favoured at pH < pH_{pzc} where the surface becomes positively charged [42].

Batch Adsorption Experiments

Effect of adsorbent dosage

The study of adsorbent dosage is important to determine the capacity of an adsorbent for a given initial concentration of dye in solution. The influence of adsorbent dosage on the removal of MB from aqueous solution was studied using variable amounts of CCS-AC ranging from 0.02 to 0.50 g. The result for adsorptive removal of MB with respect to adsorbent dosage is presented in Fig. 4.

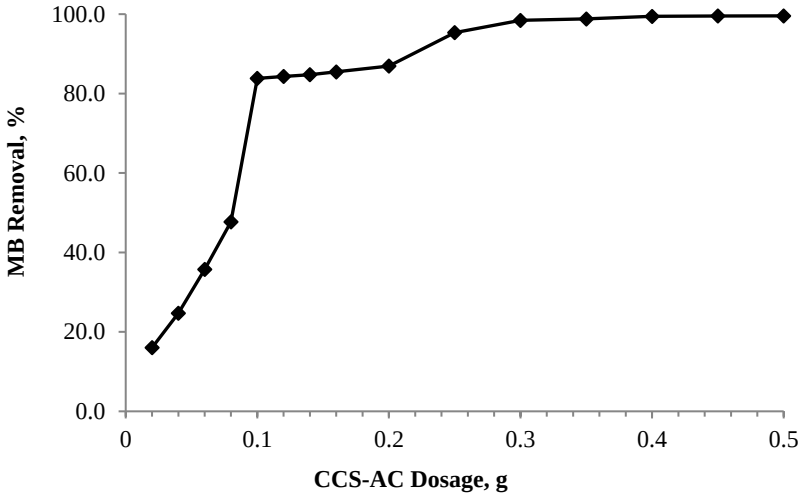

Figure 4: Effect of CCS-AC dosage on MB removal (%) at $[MB]_o$ = 100 mgL^{-1}, V = 100 mL, pH = non-adjusted (5.8 ± 0.2), T = 303 K, shaking speed = 110 stroke/min and contact time = 2 hours

It is obvious that the percentage removal of MB increases rapidly with increase of CCS-AC dosage due to the greater availability of the exchangeable sites or surface areas [43-45]. The highest level of MB removal was achieved at CCS-AC dose of 0.25 g/100 mL with 95.36% and thereafter, further increase of dosage did not exert any significant changes. This situation can be explained by an aggregate formation during adsorption, which takes place at high adsorbent concentrations causing a decrease in the effective adsorption areas [46]. Therefore, in the further experiments, the CCS-AC dosage was fixed at 0.25 g in 100 mL of MB aqueous solution.

Effect of pH

The pH of solution was expected to influence the adsorption capacity of dyes as it has the ability to modify dyes chemistry and also the surface charge of the adsorbent. Fig. 5 shows that MB uptake by CCS-AC was not affected by pH within the range from 3 to 10. Similar observations have been described for the adsorption of MB by *Parthenium hysterophorus* [47], *Prosopis cineraria* sawdust [48], *Posidonia oceanica (L.)* fibers [49], *Punica granatum* peels [50] and coconut leaves [7, 51, 52, 53].

Generally, at acidic pH, the surface of adsorbent is positively charged, making (H+) ions compete effectively with cations from dyes, causing a decrease in the amount of dyes adsorbed. Meanwhile, at alkaline pH, the surface of adsorbent adopts negative surface charge, hence, improved the uptake of positively charged dyes species via attractive electrostatic attraction, in accordance with an increase in the rate of adsorption. Therefore, in this work, the pH of MB solution was fixed at non-adjusted pH (5.8 ± 0.2) in further adsorption studies herein.

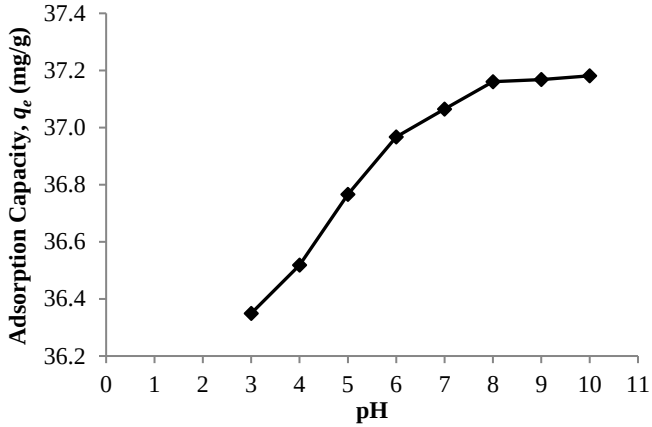

Figure 5: Effect of pH on the adsorption capacity of MB by CCS-AC at $[MB]_o$ = 100 mgL^{-1}, V = 100 mL, T = 303 K, shaking speed = 110 stroke/min, contact time = 2 hours and CCS-AC dosage = 0.25 g

Effect of initial dye concentrations and contact time

The effect of concentrations and contact time is crucial for determining the time required for the adsorbent to achieve equilibrium. Fig. 6 displayed the graph between the amounts of MB adsorbed (q_t) versus t (min) at different MB concentrations. The time variation plot pointed that the adsorption of MB was fast at the initial stages. However, once equilibrium was nearly approached, the adsorption gradually slowed down. This situation may be due to the availability of unfilled active sites during the beginning stage of adsorption, and after certain period of time, vacant sites get occupied by MB molecules, creating a repulsive force between MB and CCS-AC surface in bulk phase. The amount of MB adsorbed by the CCS-AC at equilibrium improved from 5.69 mgg^{-1} to 148.66 mgg^{-1} as the initial MB concentration increased from 25 to 400 mgL^{-1}.

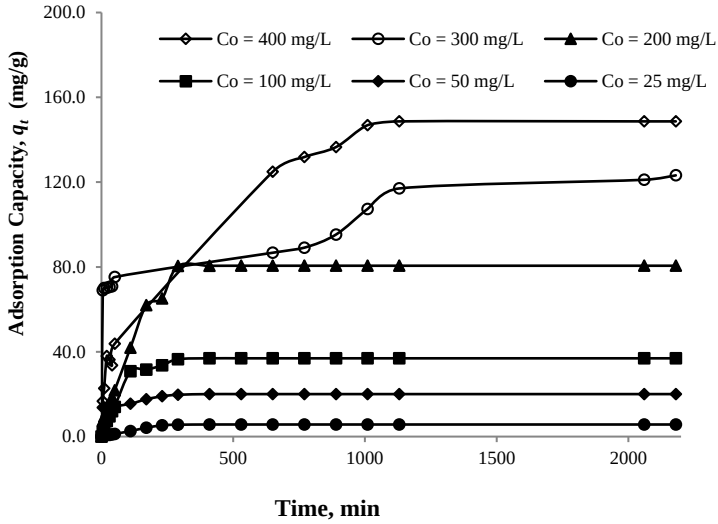

Figure 6: Effect of initial concentration and contact time on the adsorption capacity of MB by CCS-AC at V = 100 mL, T = 303 K, pH = non-adjusted (5.8 ± 0.2), shaking speed = 110 stroke/min and CCS-AC dosage = 0.25 g

In batch adsorption experiments, the removal rate of the dyes from aqueous solutions is controlled by the transport of dyes molecules from the surrounding sites to the interior sites of the adsorbent. A high MB concentration not only provides a large driving force to overcome all mass transfer resistances between the aqueous and solid phases, but also determines a higher probability of collision between MB ions and CCS-AC surface. At higher MB concentrations, longer time was required for adsorption to complete since there is a probability for MB molecules to penetrate deeper within the interior surface of the CCS-AC and be adsorbed at active pore sites.

Adsorption Isotherm

Adsorption isotherm is useful to predict the interaction between the amount of adsorbate adsorbed by adsorbent and the adsorbate concentration remaining in the solution once the system achieved an equilibrium state [54]. Three isotherm models; Langmuir [55], Freundlich [56] and Temkin [57] were tested in this work. Parameters obtained from the different models provide information on the sorption mechanisms, surface properties and affinities of the adsorbent.

Langmuir model is based on the assumption that adsorption occurs at surface with specific homogenous sites, equivalent sorption energies and no interactions between adsorbed species [35]. It explains monolayer adsorption, which lies on the fact that no further adsorption takes place once the active sites are covered with adsorbate molecules. The monolayer isotherm model is presented by the following mathematical relation (3):

$$\frac{C_e}{q_e} = \frac{1}{q_{\max} k_L} + \frac{1}{q_{\max}} C_e \qquad (3)$$

where C_e is the equilibrium concentration (mgL^{-1}) and q_e is the amount adsorbed species per specified amount of adsorbents (mgg^{-1}), k_L is the Langmuir equilibrium constant and q_{max} is the amount of adsorbate required to form an adsorbed monolayer. Hence, a plot of C_e/q_e versus C_e should be a straight line with a slope ($1/q_{max}$) and an intercept as ($1/q_{max}.k_L$). Freundlich model is based on the assumption that multilayer adsorption process takes place on heterogeneous adsorption sites. Linear equation of Freundlich model is presented as Eq. (4):

$$\ln q_e = \ln k_F + \frac{1}{n} \ln C_e \qquad (4)$$

where C_e is the equilibrium concentration of the adsorbate (mgL^{-1}), q_e is the amount of adsorbate adsorbed per unit mass of adsorbents (mgg^{-1}). The plot of *ln* q_e versus *ln* C_e yields a straight line with slope of *1/n*. k_F is calculated from the intercept value. k_F and *n* are Freundlich constants which related to maximum adsorption capacity ((mg/g) (L/mg)1/n) and adsorption intensity respectively. The slope of *1/n* ranging between 0 and 1 is a measure of adsorption intensity or surface heterogeneity, becoming more heterogeneous as its value gets closer to zero. Temkin model assumes that the heat of adsorption of all the molecules in the layer decreases linearly with coverage due to adsorbent/adsorbate interactions, and adsorption is characterized by a uniform distribution of binding energies, up to some maximum binding energy. Temkin isotherm can be expressed in its linear form and presented as Eq. (5) below:

$$q_e = B \ln k_T + B \ln C_e \qquad (5)$$

where $B = (RT/b)$, a plot of q_e versus $ln\ C_e$ yielded a linear line enables to determine the isotherm constants k_T and B. k_T is the Temkin equilibrium binding constant (Lmg^{-1}) that corresponds to the maximum binding energy and constant B is related to heat of adsorption. Linear plots of Langmuir, Feundlich and Temkin models are shown in Figs. 7 (a,b,c), respectively and the isotherm related parameters are shown in Table 2.

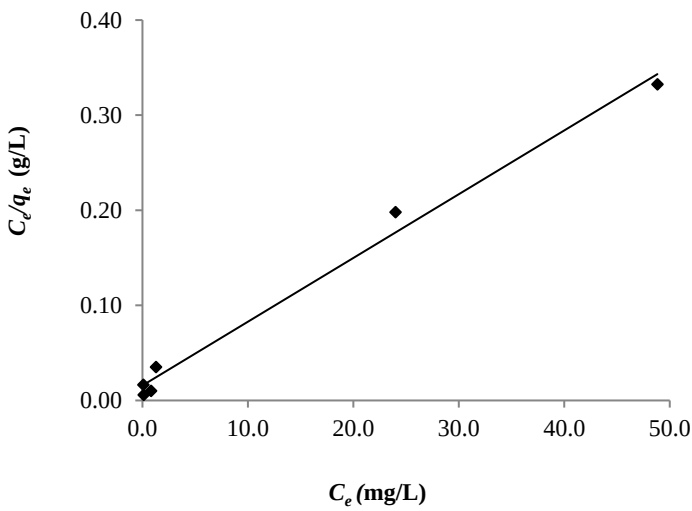

Figure. 7: Isotherm models for the adsorption of MB onto CCS-AC (a) Langmuir (b) Freundlich (c) Temkin

Table 2: Isotherm parameters for removal of MB by CCS-AC at 303 K

Isotherm	Parameters	Values
Langmuir	q_{max} (mgg^{-1})	149.25
	k_L (Lmg^{-1})	0.427
	R^2	0.999
Freundlich	K_F [$(mg/g)\ (L/mg)^{1/n}$]	35.53
	$1/n$	0.42
	R^2	0.78
Temkin	B	121.31
	k_T (Lmg^{-1})	17.50
	R^2	0.906

Based on the calculated data, Langmuir model was best fitted with the highest correlation coefficients, R^2 compared with the Freundlich and Temkin models. This proved that the homogeneous and monolayer coverage of MB has occurred on the CCS-AC surface. The CCS-AC surface is made up of small adsorption patches, which are energetically equivalent to each other in terms of adsorption phenomenon. The maximum monolayer adsorption capacity ($q_{max)}$ for CCS-AC with MB was compared with different coconut-based AC as tabulated in Table 3.

Table 3: Comparison of maximum adsorption capacities of MB using different type of coconut-based AC

Materials	Activator	Dosage, g/100mL	pH	Temp. (K)	q_{max} (mg/g)	Ref.
Commercial coconut shell	-	0.25	5.8 ±0.2	303	149.25	This Study
Coconut husk	KOH	0.10	Non-adjusted	303 313 323	434.78 416.67 384.62	[58]
Coconut leaves	H_3PO_4	0.06	5.8 ±0.2	303 313 323	357.14 370.37 370.37	[7]
Coconut leaves	KOH	0.10	5.8 ±0.2	303 313 323	147.1 151.5 151.5	[52]
Coconut leaves	H_2SO_4	0.15	5.8 ±0.2	303 313 323	126.9 137.0 137.0	[51]
Coconut leaves	$FeCl_3$	0.10	5.8 ±0.2	303	66.00	[53]

Adsorption Kinetic

Adsorption kinetic was studied in order to understand the rate controlling mechanism of adsorption such as mass transfer and chemical reactions processes. Two types of kinetic models; Pseudo First Order (PFO) and Pseudo Second Order (PSO) model were used to test the fit of the experimental data of MB uptake by CCS-AC. PFO was proposed by Lagergren [59] and considers the rate of occupation of sorption sites to be proportional to the number of unoccupied sites. Its linearized form is given by Eq. (6):

$$\ln(q_e - q_t) = \ln q_e - k_1 t \qquad (6)$$

where k_1 (1/min) is the rate constant of PFO model, q_e (mgg^{-1}) is the amount of equilibrium uptake and q_t (mgg^{-1}) is the amount of solute adsorbed at any t (min). q_e and k_1 values at different initial MB concentrations were calculated from the plots of $ln(q_e-q_t)$ against t (Fig. 8a). The linear form of the PSO model is given by Eq. (7) [60].

$$\frac{t}{q_t} = \frac{1}{k_2 q_e^2} + \frac{t}{q_e} \qquad (7)$$

where $h=k_2qe^2$ can be regarded as the initial adsorption rate and k^2 (mg/(min.g)) is the PSO rate constant. The values of k^2 and q_e were calculated from the intercept and slope of t/q_t versus t, respectively. The PSO rate constant k_2 and $q_{e,cal}$ were calculated from the intercept and slope of t/q_t against t, as shown in Fig. 8b.

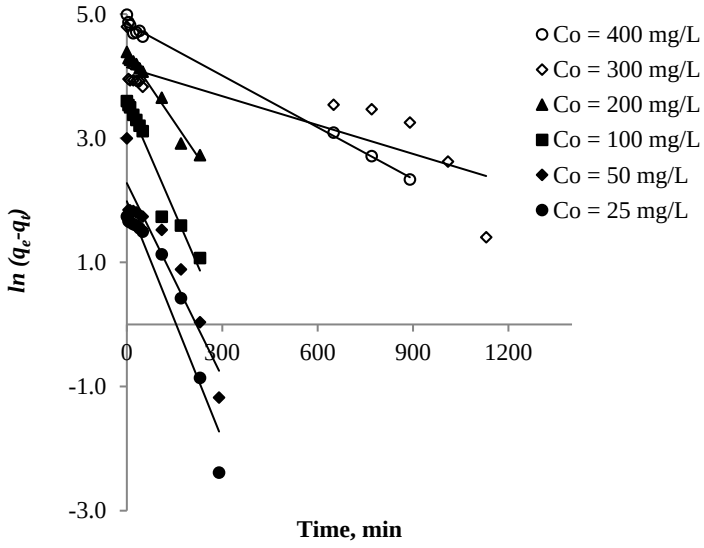

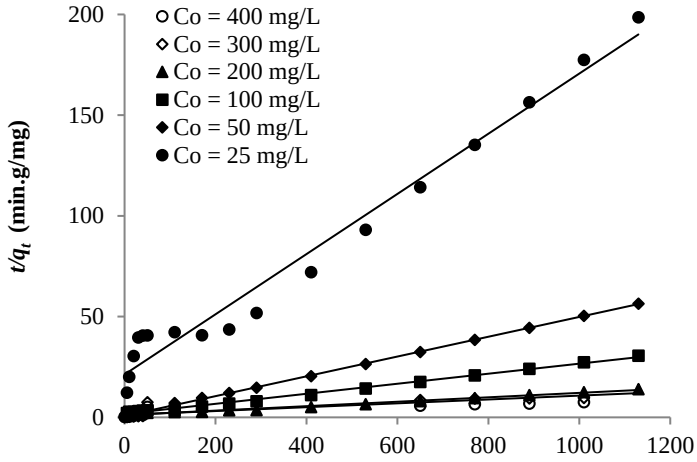

Figure 8: Kinetic profiles for the adsorption of MB onto CCS-AC (a) Pseudo First Order and (b) Pseudo Second Order

As referred in Table 4, the observed R^2 values were nearly unity ($R^2 \geq$ 0.99) for the PSO kinetic model, where the values of $q_{e,cal}$ are in good agreement with $q_{e,exp}$. This suggests that the adsorption systems studied possess chemisorption in which the attraction forces between MB molecules and the CCS-AC surface are due to chemical bonding. Chemisorption occurs only as a monolayer and substances chemisorbed on solid surface are hardly removed because of stronger forces at stake [37].

Table 4: Comparison of the PFO and PSO model for the adsorption of MB by CCS-AC at 303 K

Parameter	Concentration, C_o (mg/L)					
	25	50	100	200	300	400
$q_{e,\,exp}$ (mg/g)	5.69	20.03	36.91	80.57	117.03	148.66
PFO						
$q_{e,\,cal}$ (mg/g)	7.27	9.74	36.09	80.46	68.59	126.72
$k_{1\times}\,10^{-2}$	1.28	1.04	1.18	0.75	0.60	0.28
R^2	0.925	0.954	0.984	0.887	0.947	0.858
PSO						
$q_{e,\,cal}$ (mg/g)	7.65	15.34	49.26	99.71	125.00	138.89
$k_{2\times}\,10^{-3}$	0.90	6.76	0.26	0.10	0.29	0.10
R^2	0.971	1.000	0.994	0.986	0.978	0.989

Adsorption Thermodynamics

Thermodynamic parameters provide information about energetic changes associated with adsorption. The thermodynamic parameters of MB removal by CCS-AC were determined by carrying out the adsorption experiments at 303, 313 and 323 K. Thermodynamic constants; standard Gibbs free energy change ($\Delta G°$), standard enthalpy change ($\Delta H°$) and standard entropy change ($\Delta S°$) were calculated using the following equation **[**61**]**:

$$k_d = \frac{q_e}{C_e} \qquad (8)$$

$$\Delta G° = \Delta H^0 - T\Delta S^0 \qquad (9)$$

$$\ln k_d = \frac{\Delta S°}{R} - \frac{\Delta H°}{RT} \qquad (10)$$

where k_d is the distribution coefficient, q_e is the concentration of MB adsorbed on CCS-AC at equilibrium (mg/L), C_e is the equilibrium concentration of MB in the liquid phase (mgL^{-1}), R is the universal gas constant (8.314J/mol.K) and T is the absolute temperature (K). The values of $\Delta H°$ and $\Delta S°$ were calculated from the slope and intercept respectively from plot of $ln\ k_d$ against $1/T$ (Fig. 9).

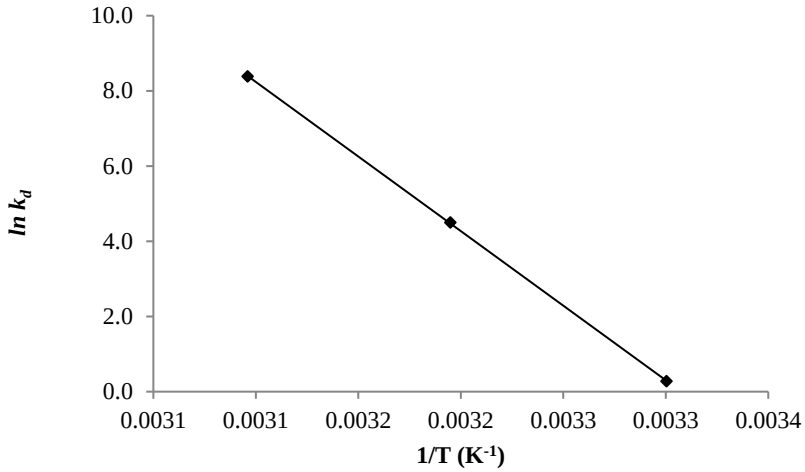

Figure 9: Plot of *ln* k_d vs. *1/T* for calculation of thermodynamic parameters for the adsorption of MB onto CCS-AC

Table 5: Thermodynamic parameters values for the adsorption of MB onto CCS-AC

Temp. (K)	Thermodynamic Parameters			
	k_d	$\Delta G°$ (kJ/mol)	$\Delta H°$ (kJ/mol)	$\Delta S°$ (J/mol K)
303	151.81	-660.35	135.17	483.03
313	141.63	-671.26		
323	4374.29	-682.17		

The thermodynamic parameters are listed in Table 5. The negative values for $\Delta G°$ point out the spontaneity of the adsorption process does not required energy from any external sources. A positive value of $\Delta H°$ suggests that the adsorption of MB onto CCS-AC surface is an endothermic in nature and follows a physisorption mechanism. A positive value $\Delta S°$ implies an increased disorder at the solid/liquid interface during the adsorption process causing the MB molecules to escape from CCS-AC surface to the liquid phase **[**62**]**. Therefore, it can be stated that the amount of MB molecules adsorbed will increase by elevating the adsorption temperature.

CONCLUSION

The research shows that CCS-AC provides a low-cost adsorbent for the removal of MB from aqueous solutions. The adsorption experiments indicated that the Pseudo Second Order model provided the best description of the kinetic uptake properties, while adsorption result at equilibrium were described by the Langmuir model with the maximum adsorption capacity (q_{max}) of 149.25 mgg^{-1}.

REFERENCES

[1] A.P. Vieira, S.A.A. Santana, C.W.B. Bezerra, H.A.S. Silva, J.A.P Chaves, J.C.P. de Melo, E.C. da Silva Filho & C. Airoldi, 2009. Kinetics and Thermodynamics of Textile Dye Adsorption from Aqueous Solutions using Babassu Coconut Mesocarp. *J. Hazard. Mater., 166*(2-3), pp. 1272–1278.

[2] M.A. Ahmad, N.A. Ahmad Puad & O.S. Bello, 2014. Kinetic, Equilibrium and Thermodynamic Studies of Synthetic Dye Removal using Pomegranate Peel Activated Carbon Prepared by Microwave-Induced KOH Activation. *Water Resour., 6*, pp. 18–35.

[3] R. Juang & S. Swei, 1996. Effect of Dye Nature on Its Adsorption from Aqueous Solution onto Activated Carbon. *Sep. Sci. Technol., 31*, pp. 2143–2158.

[4] A.E. Ofomaja & Y.S. Ho, 2008. Effect of Temperatures and pH on Methyl Violet Biosorption by Mansonia Wood Sawdust. *Bioresource Technol., 99*(13), pp. 5411–5417.

[5] V. Ponnusami, S. Vikram & S.N. Srivastava, 2008. Guava (*Psidium guajava*) Leaf Powder : Novel Adsorbent for Removal of Methylene Blue from Aqueous Solutions. *J. Hazard. Mater., 152*, pp. 276–286.

[6] M.J. Ahmed & S.K. Theydan, 2012. Physical and Chemical Characteristics of Activated Carbon Prepared by Pyrolysis of Chemically Treated Date Stones and Its Ability to Adsorb Organics. *Powder Technol., 229*, pp. 237–245.

[7] A.H. Jawad, R.A. Rashid, K. Ismail & S. Sabar, 2017. High Surface Area Mesoporous Activated Carbon Developed from Coconut Leaf by Chemical Activation with H_3PO_4 for Adsorption of Methylene Blue. *Desalin. Water Treat., 74*, pp. 326–335.

[8] A.Y. Lehi & A. Akbari, 2017. Membrane Capsules with Hierarchical $Mg(OH)_2$ Nanostructures as Novel Adsorbents for Dyeing Wastewater Treatment in Carpet Industries. *J. Taiwan Inst. Chem. Eng., 70*, pp. 391–400.

[9] A.R. Khataee, A. Movafeghi, S. Torbati, S.Y. SalehiLisar & M. Zarei, 2012. Phytoremediation Potential of Duckweed (*Lemna Minor L.*) In Degradation of C.I. Acid Blue 92: Artificial Neural Network Modelling. *Ecotoxicol. Environ. Saf., 80*, pp. 291–298.

[10] L. Fan, Y. Zhou, W. Yang, G. Chen & F. Yang, 2008. Electrochemical Degradation of Aqueous Solution of Amaranth Azo Dye on ACF under Potentiostatic Model. *Dyes Pigments, 76*, pp. 440–446.

[11] J.S. Wu, C.H. Liu, K.H. Chu & S.Y. Suen, 2008. Removal of Cationic Dye Methyl Violet 2B from Water by Cation Exchange Membranes. *J. Membr. Sci., 309*, pp. 239–245.

[12] Y.S. Woo, M. Rafatullah, A.F.M. Al-Karkhi & T.T. Tow, 2013. Removal of Terasil Red R Dye by using Fenton Oxidation: A Statistical Analysis. *Desal. Water Treat., 53*, pp. 1–9.

[13] A.H. Jawad, A.F.M. Alkarkhi & N.S.A. Mubarak, 2015. Photocatalytic Decolorization of Methylene Blue by an Immobilized TiO_2 Film under Visible Light Irradiation: Optimization using Response Surface Methodology (RSM). *Desalin. Water Treat., 56*, pp. 161–172.

[14] A.H. Jawad, N.S A. Mubarak, M.A.M. Ishak, K. Ismail & W.I. Nawawi, 2016. Kinetics of Photocatalytic Decolourization of Cationic Dye using Porous TiO_2 Film. *J. Taibah Univ. Sci., 10*, pp. 352–362.

[15] A. Bhatnagar, M. Sillanpää & A. Witek-krowiak, 2015, Agricultural Waste Peels as Versatile Biomass for Water Purification–A Review. *Chem. Eng. J., 270*, pp. 244–271.

[16] A.H. Jawad, M.A. Islam & B.H. Hameed, 2017. Cross-Linked Chitosan Thin Film Coated onto Glass Plate as an Effective Adsorbent for Adsorption of Reactive Orange 16. *Int. J. Biol. Macromolec., 95*, pp. 743–749.

[17] N.S.A. Mubarak, A.H. Jawad & W.I. Nawawi, 2017. Equilibrium, Kinetic and Thermodynamic Studies of Reactive Red 120 Dye Adsorption by Chitosan Beads from Aqueous Solution. *Energ. Ecol. Environ., 2*, pp. 85–93.

[18] D. Cuhadaroglu & O.A. Uygun, 2008. Production and Characterization of Activated Carbon from a Bituminous Coal by Chemical Activation. *Afr. J. Biotechnol., 7*(20), pp. 3703–3710.

[19] J. Hayashi, A. Kazehaya, K. Muroyama & A.P. Watkinson, 2000. Preparation of Activated Carbon from Lignin by Chemical Activation. *Carbon, 38*, pp. 1873–1878.

[20] J.R. Hernandez, F.L. Aquino & S.C. Capareda, 2007. Activated Carbon Production from Pyrolysis and Steam Activation of Cotton Gin Trash. *Am. Soc. Agric. Biol. Eng.*, pp. 1–8.

[21] X.J. Jin, Z.M. Yu & Y. Wu, 2010. Preparation of Activated Carbon from Lignin Obtained by Straw Pulping by KOH and K_2CO_3 Chemical Activation. *Cellul. Chem. Technol., 46*(1–2), pp. 79–85.

[22] Y. Sun, J.P. Zhang, G. Yang & Z.H. Li, 2006. Removal of Pollutants with Activated Carbon Produced From K_2CO_3 Activation of Lignin from Reed Black Liquors. *Chem. Biochem. Eng Q., 20*, pp. 429–435.

[23] A.R. Yacob, Z.A. Majid, R.S.D. Dasril & V. Inderan, 2008. Comparison of Various Sources of High Surface Area Carbon Prepared by Different Types of Activation. Malays. *J. Anal Sci., 12*, pp. 264–271.

[24] Z. Zhu, A. Li, M. Xia, J. Wan & Q. Zhang, 2008. Preparation and Characterization of Polymer Based Spherical Activated Carbons. *Chin. J. Polym. Sci., 26,* pp. 645–651.

[25] Z. Hu & M.P. Srinivasan, 2001. Mesoporous High Surface Area Activated Carbon. *Micro Meso Mater., 43*, pp. 267–275.

[26] S. Guo, J. Peng, W. Li, K. Yang, L. Zhang & S. Zhang, 2009. Effects of CO_2 Activation on Porous Structures of Coconut Shell-Based Activated Carbons. *Appl. Surf. Sci., 255*(20), pp. 8443–8449.

[27] J.N. Sahu, J. Acharya & B.C. Meikap, 2010. Optimization of Production Conditions for Activated Carbons from Tamarind Wood by Zinc Chloride using Response Surface Methodology. *Bioresour. Technol., 101*, pp. 1974–1982.

[28] J.M. Dias, M.C.M. Alvim-Ferraza, M.F. Almeida, J. Rivera-Utrilla & M. Sanchez-Polo, 2007. Waste Materials for Activated Carbon Preparation and Its use in Aqueous-Phase Treatment: A Review. *J. Environ. Manag., 85*(4), pp. 833–846.

[29] A.M. Khah & R. Ansari, 2009. Activated Charcoal: Preparation, Characterization and Applications: A Review Article. *Int. J. Chem. Technol. Res., 1*, pp. 859–864.

[30] Y.S. Ho, R. Malaryvizhi & N. Sulochana, 2009. Equilibrium Isotherm Studies of Methylene Blue Adsorption onto Activated Carbon Prepared from *Delonix regia* Pods. J. *Environ. Prot. Sci., 3,* pp. 111–116.

[31] S. Idris, Y.A. Iyaka, B.E.N. Dauda, M.M. Ndamitso & M.T. Umar, 2012. Kinetic Study of Utilizing Groundnut Shell as in Adsorbent In; Removing Chromium and Nickel from Dye Effluent. *Am. Chem. Sci. J., 2*, pp. 12–24.

[32] Z. Al-Qodah & R. Shawabkah, 2009. Production and Characterization of Granular Activated Carbon from Activated Sludge. Braz. *J. Chem. Eng., 26*, pp. 127–136.

[33] A.L. Cazetta, A.M.M. Vargas, E.M. Nogami, M.H. Kunita, M.R. Guilherme, A.C. Martins & V.C. Almeida, 2011. NaOH-Activated Carbon of High Surface Area Produced from Coconut Shell: Kinetics and Equilibrium Studies from the Methylene Blue Adsorption. *Chem. Eng. J., 174*(1), pp. 117–125.

[34] M. Rafatullah, O. Sulaiman, R. Hashim & A. Ahmad, 2010, Adsorption of Methylene Blue on Low-Cost Adsorbents: A Review. *J. Hazard. Mater., 177*(1–3), pp. 70–80.

[35] M.V. Lopez-Ramon, F. Stoeckli, C. Moreno-Castilla & F. Carrasco-Marin, 1999. On the Characterization of Acidic and Basic Surface Sites on Carbons by Various Techniques. *Carbon, 37*, pp. 1215–1221.

[36] M. Balakrishnan & Y. Satyawali, 2007. Removal of Color from Biomethanated Distillery Spentwash by Treatment with Activated *Carbons. Bioresource Technol., 98*, pp. 2629–2635.

[37] S. De Gisi, G. Lofrano, M. Grassi & M. Notarnicola, 2016. Characteristics and Adsorption Capacities of Low-Cost Sorbents for Wastewater Treatment : A Review. *SUSMAT, 9*, pp. 10–40.

[38] K. Johari, N. Saman, S.T. Song, C.S. Chin, H. Kong & H. Mat, 2016, Adsorption Enhancement of Elemental Mercury by Various Surfaces Modified Coconut Husk as Eco-Friendly Low-Cost Adsorbents. *Int. Biodeterior. Biodegrad.*, *109*, pp. 45–52.

[39] N. Sharma, D.P. Tiwari & S.K. Singh, 2014. The Efficiency Appraisal for Removal of Malachite Green by Potato peel and Neem Bark: Isotherm and Kinetic Studies. *Int. J. Chem. Environ. Eng.*, *5*(2), pp. 83–88.

[40] W.M., Ibrahim, A.F., Hassan, Y.A., Asad & F. Azab, 2016. Biosorption of Toxic Heavy Metals from Aqueous Solution by *Ulva lactuca* Activated Carbon. *Egyptian Journal of Basic and Applied Sciences*, *3*(3), pp. 241–249.

[41] D. Pathania, S. Sharma & P. Singh, 2013. Removal of Methylene Blue by Adsorption onto Activated Carbon Developed from *Ficus carica* bast. Arab. *J. Chem.*, http://dx.doi.org/10.1016/j.arabjc.2013.04.021

[42] G.E. Nascimento, M.M.M.B. Duarte, N.F. Campos, O.R.S. Rocha & V.L. Silva, 2014. Adsorption of Azo Dyes using Peanut Hull and Orange Peel: A Comparative Study. *Environ. Technol., 35*, pp. 1436–1453.

[43] B. Royer, N.F. Cardoso, E.C. Lima, J.C.P. Vaghetti & R.C. Veses, 2009. Applications of Brazalin Pine-Fruit Shell in Natural and Carbonized forms as Adsorbents to Removal of Methylene Blue from Aqueous Solutions: Kinetics and Equilibrium Study. *J. Hazard. Mater.*, *164*(2-3), pp. 1213–1222.

[44] S. Karagöz, T. Tay, S. Ucar & M. Erdem, 2008. Activated Carbons from Waste Biomass by Sulfuric Acid Activation and Their use on Methylene Blue Adsorption. *Bioresour. Technol., 99*, pp. 6214–6222.

[45] C. Deng, J. Liu, W. Zhou, Y.K. Zhang, K.F. Du & Z.M. Zhao, 2012. Fabrication of Spherical Cellulose/Carbon Tubes Hydrid Adsorbent Anchored with Welan Gum Polysaccharide and its Potential in Adsorbing Methylene Blue. *Chem. Eng. J., 200–202*, pp. 452–458.

[46] G. Crini & P. M. Badot, 2008. Application of Chitosan, a Natural Aminopolysaccharide, For Dye Removal from Aqueous Solutions by Adsorption Processes using Batch Studies: A Review of Recent Literature. *Prog. Polym. Sci., 33*(4), pp. 399–447.

[47] H. Lata, V.K. Garg & R.K. Gupta, 2007. Removal of a Basic Dye from Aqueous Solution by Adsorption using *Parthenium hysterophorus*: An Agricultural Waste. *Dyes Pigm., 74*(3), pp. 653–658.

[48] V.K. Garg, R. Kumar & R. Gupta, 2004. Removal of Malachite Green Dye from Aqueous Solution by Adsorption using Agro-Industry Waste: A Case Study of *Prosopis cineraria*. *Dyes Pigments, 62*, pp. 1–10.

[49] M.C. Ncibi, B. Mahjoub & M. Seffen, 2007. Kinetic and Equilibrium Studies of Methylene Blue Biosorption by *Posidonia oceanica (L.)* Fibres. *J. Hazard. Mater., 139*, pp. 280–285.

[50] A.H. Jawad, A.S. Waheeb, R.A. Rashid, W.I. Nawawi, and E. Yousif, 2018. Equilibrium Isotherms, Kinetics, and Thermodynamics Studies of Methylene Blue Adsorption on Pomegranate (*Punica granatum*) Peels as a Natural Low–Cost Biosorbent. *Desalin. Water Treat., 105*, pp. 322–331.

[51] A.H. Jawad, R.A. Rashid, M.A.M. Ishak & L.D. Wilson, 2016. Adsorption of Methylene Blue onto Activated Carbon Developed from Biomass Waste by H_2SO_4 Activation: Kinetic, Equilibrium and Thermodynamic Studies. *Desalin. Water Treat., 57*, pp. 25194–25206.

[52] R.A. Rashid, A.H. Jawad, M.A.M. Ishak & N.N. Kasim, 2016. KOH-Activated Carbon Developed from Biomass Waste: Adsorption Equilibrium, Kinetic and Thermodynamic Studies for Methylene Blue Uptake. *Desalin. Water Treat., 57*, pp. 27226–27236.

[53] R.A. Rashid, A.H. Jawad & N.N. Kasim, 2018. $FeCl_3$-Activated Carbon Developed from Coconut Leaves: Characterization and Application for Methylene Blue Removal. *Sains Malaysiana, 47*(3), pp. 603–610.

[54] V.O. Njoku, M.A. Islam, M. Asif & B.H. Hameed, 2014. Preparation of Mesoporous Activated Carbon from Coconut Frond for the Adsorption of Carbofuran Insecticide. *J. Anal. Appl. Pyrol., 110*(1), pp. 172–180.

[55] I. Langmuir, 1918. The Adsorption of Gases on Plane Surfaces of Glass, Mica and Platinum. *J. Am. Chem. Soc., 40*, pp. 1361–1403.

[56] H. Freundlich, 1906. Ueber die adsorption in Loesungen (Adsorption in solution). *Z. Phys. Chem., 5*, pp. 385–470.

[57] M.J. Temkin & V. Pyzhev, 1940. Recent Modifications to Langmuir Isotherms. Acta Physiochim. *USSR, 12*, pp. 217–222.

[58] I.A.W. Tan, A.L. Ahmad & B.H. Hameed, 2008. Adsorption of Basic Dye on High Surface Area Activated Carbon Prepared from Coconut Husk: Equilibrium, Kinetic and Thermodynamic Studies. *J. Hazard. Mater., 154*(1-3), pp. 337–346.

[59] S. Lagergren, 1898. Zurtheorie der Sogenannten Adsorption Geloesterstoffe. In: Kungliga Svenska Vetenskapsakad. *Handlingar, 24*, pp. 1–39.

[60] Y.S. Ho & G. McKay, 1998. Sorption of Dye from Aqueous Solution by Peat. *Chem. Eng. J., 70*, pp. 115–124.

[61] J.J. Gao, Y.B. Qin, T. Zhou, D.D. Cao, P. Xu, D. Hochstetter & Y.F. Wang, 2013. Adsorption of Methylene Blue onto Activated Carbon Produced from Tea (*Camellia sinensis L.*) Seed Shells: Kinetics, Equilibrium, and Thermodynamics Studies. *J. Zhejiang Univ. Sci. B, 14*(7), pp. 650–658.

[62] I.A.W. Tan, A.L. Ahmad & B.H. Hameed, 2008. Adsorption of Basic Dye using Activated Carbon Prepared from Oil Palm Shell: Batch and Fixed Bed Studies. *Desalination, 225*, pp. 13–28.